Environmental Science and Pollution Research (2019) 26:26159–26169
https://doi.org/10.1007/s11356-019-05879-4

RESEARCH ARTICLE

A comparative study of using barberry stem powder and ash as adsorbents for adsorption of humic acid

Maryam Khodadadi[1,2] · Tariq J. Al-Musawi[3] · Mohammad Kamranifar[2] · Mohammad Hossein Saghi[4] · Ayat Hossein Panahi[1]

Received: 23 March 2019 / Accepted: 1 July 2019 / Published online: 6 July 2019

Abstract

In the present research, investigation of the practical utility of barberry stem powder (BSP) and barberry stem ash (BSA) for humic acid (HA) removal from an aqueous medium by adsorption was carried out. The adsorption process was tested by varying of pH (3–11), reaction time (5–20 min), initial HA concentration (5–40 mg/L), adsorbent dosage (1–4 g/L), and temperature (15–35 °C). The isothermal results revealed that the adsorption process is favorable for both used adsorbents and it is highly described using the Freundlich and Langmuir models ($R^2 > 0.960$). Also, the maximum uptakes of BSP and BSA for HA were 20.220 and 16.950 mg/g at the abovementioned optimized conditions (pH = 7, reaction time = 10 min, temperature = 15 °C, initial HA concentration = 40 mg/L, and adsorbent amount = 1.0 g/L), respectively. The results achieved from the fitting of the experimental data with Dubinin-Radushkevich isotherm model showed that the HA molecules are adsorbed onto the BSP and BSA by physiosorption process. From the thermodynamic study, it appeared that the biosorption process of the HA onto two studied adsorbents was of exothermic nature. The kinetics of the adsorption process of HA has been found to be pseudo-second-order model (R^2 = 0.930–0.999). Thus, the results obtained from this paper elucidated that the BSP exhibited higher adsorption capacity in comparison to BSA, for HA removal up to permissible concentrations.

Keywords Barberry stem · Ash · Humic acid · Adsorption mechanism · Environmental conditions

Introduction

Natural humic substances are a mixture of organic chemicals including humic acid (HA), folic acid, amino acids, hydrophilic acid, protein, lipids, and hydrocarbons compounds. The presence of these substances in the water bodies poses several critical health problems in many societies especially when the water body, has been taken into consideration for the production of the drinking water, due to their affinity towards carcinogenic disinfection by-products produced during disinfection process of water. Furthermore, color, taste, and odor are the three most common problems coming from elevated concentrations of organic matters in water (Low et al. 2008, Gasser et al. 2008). Moreover, the heavy metals, which are mostly dangerous and carcinogenic, may combine with the organic compounds present in water wing leading to their transmission into the water resources. Far from these drawbacks, the organic material in itself may form biofilms within the water distribution network pipelines (Liu et al. 2008).

Among the organic matters, the HA is one of the main subclasses of the humic matters, which forms nearly 90% of the natural organic matter, having a variety of hydrophobic and hydrophilic matters like phenol, quinone, catechol, and sugar moieties (Bazrafshan et al. 2012; Naghizadeh et al. 2013). Figure 1 depicts the chemical structure of HA molecule. HA in water purification processes is viewed as a precursor of disinfection by-product materials named as trihalomethanes (THMs) and haloacetic acids (HAA) (Babi et al.

Responsible editor: Tito Roberto Cadaval Jr

✉ Ayat Hossein Panahi
ayatpanahi@yahoo.com

[1] Social Determinants of Health Research Center, Birjand University of Medical Sciences, Birjand, Iran

[2] Medical Toxicology and Drug abuse Research Center (MTDRC), Birjand University of Medical Sciences (BUMS), Birjand, Iran

[3] Department of Civil Engineering, Faculty of Engineering, Isra University, Amman, Jordan

[4] Department of Environmental Health Engineering, School of Public Health, Sabzevar University of Medical Science, Sabzevar, Iran

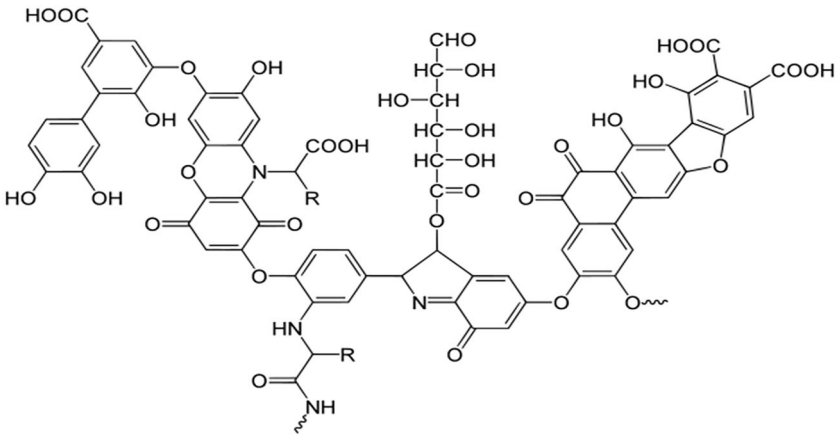

Fig. 1 Schematic representation of the HA chemical structure (Naghizadeh et al. 2016)

2007). Further, it has been scientifically established that the vital problems of THM and HAA compounds for human include toxicity, carcinogenicity, and mutagenicity, along with the damage caused by these compounds to the kidney and bladder (Dehghani et al. 2015; Babi et al. 2007). For that reason, the Environmental Protection Agency (EPA) set a strict limit on the allowed concentrations of THMs and HAA in drinking water which are suggested to be less than 80 and 60 μg/L, respectively (Uyak et al. 2008). Therefore, due to their toxic and mutagenic properties, HA compounds have gained tremendous attention by researchers for their successful removal from water and wastewater prior to disinfection (Mansoury et al. 2015).

Several studies showed that the treatment technologies used for removal of water disinfection by-products post-formation are considered to be of high cost. Therefore, considering the above limitation, scientists are putting in tremendous efforts to identify an alternative treatment method for effective prevention of the formation of these compounds through the removal of their precursors especially HA (Zhang and Minear 2006). In this field, various treatments have been suggested for removal of this precursor from water, which includes (i) advanced oxidation, (ii) biodegradation, (iii) membrane techniques, and (iv) photocatalyst (Li et al. 2017; Selcuk and Bekbolet 2008). Nevertheless, these procedures are gradually replaced by other processes since they impart a few disadvantages. The principal disadvantage is that they may produce secondary pollutants as well as they are not efficient if the concentration of the pollutant is low. Recently, other water treatment techniques were proposed, as an alternative method for HA removal that does not imply the abovementioned limitations and is simple in design and operation. Among them, the adsorption process was recommended as a successful alternative treatment method for the removal of the contaminants present in water and wastewater (Mohammed et al. 2018). In the adsorption process, two fundamental terminologies should be known. The solid material on which the adsorption process happens is called an adsorbent, and the pollutant molecule present in a solution, which gets accumulated at the surface of the solid material, is called an adsorbate (Noroozi et al. 2018; Mohseni-Bandpi et al. 2016).

Indeed, using adsorption techniques for HA removal have been validated by several studies to be efficient and simple (Hassani et al. 2015; Malakootian and Kalankesh 2014; Ngah et al. 2011; Wang et al. 2008). Recently, several natural and artificial sorbents, including (a) activated carbon (Doulia et al. 2009), (b) chitosan (Dong et al. 2014), (c) natural zeolite modified with TiO_2 (Liu et al. 2014), (d) polyaniline (Wang et al. 2014), (e) magnetic graphene oxide (Zhang et al. 2016), (f) bentonite (Anirudhan and Ramachandran 2007), and (g) eggshell powder (Zulfikar et al. 2013), were tested to examine their HA removal efficiency from water or wastewater. However, some of the abovementioned materials are found to be expensive or practically ineffective. Therefore, it is necessary for recurrent investigation and development of alternative efficacious and inexpensive adsorbents for removal of harmful HA molecules. Among the several types of utilized adsorbents, agriculture and natural wastes exhibited various positive adsorptive properties that encourage their application as an adsorbent because they are inexpensive, eco-friendly, and readily available material (Sulaymon et al. 2014). Although the agriculture wastes and natural adsorbents were identified as potential adsorbents in the adsorption systems to be efficient in the remediation of several pollutants, currently, a few numbers of papers that examined the applicability of barberry stem powder (BSP) or barberry stem ash (BSA) in the adsorption systems for the treatment of wastewater loaded with HA, have been observed. Indeed, BSP and BSA are inexpensive and nonhazardous materials. In the case of BSP, this material is easily available in nature which in turn makes it a promising biosorbent for the eradication of several hazardous materials from wastewater. In addition, the application of BSP and BSA biosorbents in the wastewater treatment systems has an added environmental advantage of reusing the solid waste generated from the agricultural fields, which in turn made them as eco-friendly materials. Therefore, the

current investigation aims to examine the feasibility of utilizing these two types of wastes as adsorbents media for HA removal from an aqueous solution. Other environmental factors that affect the adsorption mechanism, like pH, reaction time, the concentration of the pollutant, adsorbent dosage, and temperature, were also investigated. The isothermal, kinetic, and thermodynamic adsorption mechanisms were extensively studied and modeled using well-defined mathematical models.

Materials and Methods

Adsorbents

The collection of raw barberry stems used in this work was carried out using hands from several public gardens in Birjand city, Iran. Initially, the collected quantity was thoroughly washed with tap water and then with distilled water to eliminate any adhering dirt, debris, and foreign matters. The suspension was decanted followed by the removal of the supernatant. The cleansed wetted stems were oven-dried at 105 °C to obtain complete dry material. Subsequently, the dried material was grinded, powdered, and sieved to size < 500 μm. The prepared BSP was finally stored in non-venting desiccators container before being used directly in the characterization and adsorption experiments or for preparation of barberry stem ashen material. The BSA was prepared, by burning some dried barberry stems at 600 °C for 1.5 h, and the BSA left at the end of burning were cooled down at ambient temperature. Afterward, the prepared BSA was kept in a special container to ensure it does not get moistened.

Chemicals

The analytical grade HA stock solution of 500 mg/L concentration and 60% purity was supplied, by Acros Company (part of Thermo Fisher Scientific company). The stock solution was kept in a refrigerator and used for preparing the working solution for a maximum period of 2 weeks. The pH values were controlled using 0.1 M H_2SO_4 or 0.1 N NaOH purchased from Merck (Germany).

Experiments and models

Experimental work

The experimental work was conducted in batch tests using several glass beakers filled with 100 mL of the predefined concentration of HA solution. To optimize the adsorption conditions in the isotherm and kinetic experiments, the HA adsorption process onto two adsorbent used here, were investigated by varying the pH (3–11), reaction time (up to 120 min), HA initial concentration (5–40 mg/L), adsorbent dose (1–4 g/L), and temperature (15–35 °C). For the effect of pH study, five beakers with 100 mL of 20 mg/L HA solution were adjusted to initial pH of 2, 5, 7, 9, and 11. To each beaker, 0.2 g of BSP or BSA was added and allowed to equilibrate initially for 60 min. The effects of the reaction time from inception to 120 min on the biosorption activity of BSP or BSA were studied simultaneously with the variation of the initial HA concentrations at 5, 10, 20, 30, and 40 mg/L. The initial pH of the HA solutions was fixed at the optimized value from the previous experiment. To study the effect of BSP and BSA dose on the biosorption mechanism, different amounts of each biosorbent (0.1, 0.2, 0.3, and 0.4 g) were shaken with 100 mL HA solution of 40 mg/L and pH = 7. The thermodynamic study was conducted using three beakers containing 100 mL of 40 mg/L HA solution. The temperature was fixed at 15, 25, and 35 °C while the other parameters were fixed at the optimized values resulted from the previous experimental work.

The shaking of the beakers was performed using an incubator shaker (Model SI-100R, Korea) with a constant speed of 250 rpm, to reach the equilibrium selected from the effect of reaction time experiment. The results of the repercussions of the adsorbent dose, reaction time, and temperature were employed for the isotherm, kinetic, and thermodynamic studies, respectively. At the end of each test, 2.0 mL of samples was withdrawn, immediately filtered, centrifuged, and then tested for their remaining of HA concentration using a UV/VIS spectrometer ($T80^+$, PG Instrument Ltd). Further, the analysis of all the experimental samples was carried out in duplicate, and the average results were determined. The adsorption capacity (q_e, mg/g) of the BSP and BSA for HA could be calculated using Eq. 1 (Li et al. 2017), which is written as:

$$q_e = \frac{V}{m} \times (C_o - C_e) \quad (1)$$

where C_o and C_e are denoted to the concentrations of the HA (mg/L) at initial (before adsorption) and equilibrium time, respectively, V is the sample volume (L), and m is the mass of the used adsorbent (g).

Isotherm models

As well described by several adsorption studies, the equilibrium isotherm is one of the vital features that offer accurate understanding regarding the study of the adsorption of contaminants on different adsorbents (Mohammed et al. 2018; Hassani et al. 2015;). In this research, the experimental data of equilibrium between adsorbed and free HA molecules in the aqueous solutions were fitted using the models of Freundlich, Langmuir, BET, Temkin, and Dubinin-Radushkevich.

The Freundlich model is expressed in the exponential form (Eq. 2) (Freundlich 1906). This model proposes a non-uniform distribution of the adsorption energy over the heterogeneous adsorbent sits. Additionally, this model is found to be the best representative to multilayer systems, where the adsorption surface site gets saturated with more than one adsorbate molecule. Notably, K_f in Freundlich model is a constant, which represents the extent of the adsorption and its magnitude provides quantitative information about the affinity of the adsorbent toward the adsorbate (Freundlich 1906), whereas the surface heterogeneity is characterized using the empirical coefficient (n) in which the surface of the adsorbent becomes more heterogeneous as n^{-1} value approaches to zero.

$$q_e = K_f C_e^{\frac{1}{n}} \tag{2}$$

The generalized non-linear form of the Langmuir isotherm model under constant temperature equilibrium is stated, as Eq. (3). Indeed, the Langmuir model is usually applied to explain the monolayer adsorption of the adsorbate molecules with a finite number of homogeneous adsorbent sits, where the adsorption surface site gets saturated with not more than one adsorbate molecule (Langmuir 1918).

$$q_e = \frac{q_{max} K_L C_e}{1 + K_L C_e} \tag{3}$$

where q_{max} is an essential parameter representing the maximum adsorption capacity of the adsorbent (mg/g), and K_L is a Langmuir constant denoting the equilibrium of adsorption (L/mg).

The Temkin model is widely used to express the behavior of the adsorption system on heterogeneous adsorption surfaces. The Temkin isotherm parameters are calculated by Eq. (4) (Doulia et al. 2009).

$$q_e = \frac{RT}{b_T} \ln(A_T C_e) \tag{4}$$

where T is absolute temperature (K), R is the universal gas constant (8.314 J/mol K), b_T is corresponding to the heat of sorption (J/mol), and A_T is the equilibrium binding constant (L/g).

The BET model (Eq. 5) assumes the adsorption phenomena occurred at multi-layer adsorption sites.

$$q_e = \frac{q_{max}\, K_b C_e}{(C_s - C_e)\left(1 + (K_b - 1)\left(\frac{C_e}{C_s}\right)\right)} \tag{5}$$

where k_b is the constant describing the energy of the interaction between adsorbent and sorbate, and C_s is the saturation concentration of the sorbate material in solution (mg/L).

The Dubinin-Radushkevich isotherm is used to express the nature of adsorption as physical and chemical. The Dubinin-Radushkevich isotherm equation is as follows (Eq. 6).

$$q_e = q_m\, e^{-\beta \varepsilon^2} \tag{6}$$

where q_m is the maximum adsorption capacity of one layer (mg/g), β is parameter denoting the mean free energy (E, kJ/mol) of adsorption (mol^2/kJ^2), and ε is the constant of the Polanyi potential (J/mol). Notably, the value of ε and E are calculated using Eqs. 7 and 8, respectively (Şeker et al. 2008).

$$\varepsilon = RT \ln\left(1 + \left(\frac{1}{C_e}\right)\right) \tag{7}$$

$$E = (2\,\beta)^{-0.5} \tag{8}$$

Kinetic models

To check the selectivity and to evaluate the adsorption performance of an adsorbent, used for the purification of the contaminant ions, the understanding of the highly complex kinetic mechanism is essential (Brouers and Al-Musawi 2018; Samarghandi et al. 2015). Moreover, the accurate design of the continuous adsorption system in the tertiary treatment units highly depends on the knowledge obtained regarding the interaction mechanism between the adsorbent–adsorbate complex (Balsamo and Montagnaro 2015). In this context, the pseudo-first- and second-order kinetic equations were widely applied to (i) model the experimental kinetic data and (ii) describe the kinetic process of adsorption. Indeed, the pseudo-first-order formula was developed according to the assumption that the one pollutant molecule occupies only one active site on the adsorbent surface. Additionally, the adsorption rate over time is directly proportional to the saturation concentration and the number of active sites, thereby following physisorption. The pseudo-second-order model supposes that the pollutant molecule can occupy more than one sorption site, which in turn indicates that the nature of the sorption mechanism is chemisorption. In the present study and to evaluate the rate of HA adsorption onto two adsorbents, the experimental kinetic data were analyzed using two well-defined models that is widely used by most studies and these are pseudo-first- and second-order models given by Eqs. (9) and (10), respectively (Lagergren 1898; Ho and Mckay 2000).

$$q_t = q_e\left(1 - e^{-k_1 t}\right) \tag{9}$$

$$q_t = \frac{k_2 q_e^2\, t}{1 + k_2 q_e t} \tag{10}$$

where q_t is the uptake of the adsorbent for adsorbate (mg/g) at reaction time t (min), and k_1 and k_2 are the rate constants of the first- and second-order kinetic models (min^{-1}), respectively.

Thermodynamic models

Eventually, to determine the thermodynamic mechanism of HA adsorption onto BSP and BSA, the thermodynamic constants of surface adsorption of entropy change ($\Delta S°$, kJ/mol K); Gibbs free energy change ($\Delta G°$, kJ/mol), and enthalpy change ($\Delta H°$, kJ/mol) were investigated using Eqs. (11)–(13) (Kamranifar and Naghizadeh 2017; Milonjic 2007; Rodrigues et al. 2018).

$$\Delta G° = -RT\ln(\rho_w.kd) \tag{11}$$

$$\ln(\rho_w.K_d) = -\frac{\Delta H°}{RT} + \frac{\Delta S°}{R} \tag{12}$$

$$\text{with} \quad K_d = \frac{q_e}{C_e} \tag{13}$$

where K_d is the equilibrium constant (L/g) defined by the ratio of the sorbed concentration of HA molecules (mg/g) and the equilibrium concentration (mg/L), ρ_w is the density of water (mg/L), and R is the universal gas constant (0.008314 kJ/mol K)

Determination of pH of point zero charge (pHpzc)

The determination of pH_{pzc} of BSP and BSA was conducted according to the detailed methodology (Mohammed et al. 2019). Thus, 16 beakers were filled with 100 mL HA solution of concentration = 40 mg/L and the initial pH values were adjusted from 3 to 10. Afterward, a specific amount of 0.5 g of dried powdered of BSP or BSA was added to each flask and the mixtures were vigorously shaken for 60 min. The pH_{pzc} was determined from the intersection point of the initial and final pH curves.

Results and discussion

Characteristics of the adsorbents

To investigate the fundamental morphological characteristics of the two adsorbents used, SEM micrographs of BSP and BSA, post and prior HA adsorption, at a scale bar of 200 nm (see Fig. 2), were captured. The SEM image of BSP (see Fig. 2a) reveals that the surface of this adsorbent consists of wrinkled layers, in addition to big cracks and ravines. Additionally, it is possible to visualize several irregular-shaped aggregates with sizes ranging from 60 to 170 nm in diameter. These significant features impart a favorable situation for HA removal by good adsorbent since these characteristics increase the surface area for the contaminants adhering. After HA adsorption (see Fig. 2b), the surface morphology of the barberry stem undergoes significant alteration. From the SEM image of the barberry stem after adsorption of HA, it is evident that the surface of the barberry stem becomes more smothered, while the brightness has reduced as well as some of the formerly distinguished aggregates and cracks also disappeared. These changes could be attributed to the covering of both the outer surface and inner pores of the barberry stem particles by HA molecules. The SEM images of barberry stem BSA, prior and post reaction with HA, are shown in Fig. 2c and d, respectively. From the micrograph of BSA (Fig. 2c), one can observe that the surface of this adsorbent is smooth and consisted of irregularly shaped combined layers. Similar to Barberry Stem, several individual particles of different size were also spread over the surface of the BSA. Moreover, after HA adsorption onto BSA (see Fig. 2d), the surface morphology of this adsorbent was distorted, which is further being characterized by non-smooth small peels with relatively large pores of different sizes. The possible reason of these changes might be the reaction of HA molecules onto BSA surface sites.

Effect of pH

Figure 3a shows the results of the analysis of pHpzc of the BSP and BSA. It can be seen that the pHpzc is observed to be approximately 7. Therefore, in solution with pH > 7, the present two bisorbents would have net negative charges on their surfaces. On the contrary, when the solution has a pH < 7, the biosorbent surfaces will have a positive charge. The results of the effects of solution pH on the adsorption of HA on two adsorbents are depicted in Fig. 3b. From the figure, it is evident that the pH value had an insignificant effect on HA removal on the two adsorbents. However, at neutral pH, relatively high adsorption capacities were determined. This significant phenomenon revealed a favorable and eco-friendly treatment method for HA removal using BSP and BSA, via adsorption, since almost all natural water bodies are within near neutral pH. At a pH value of 7, HA adsorption on BSA was 8.1 mg/g, while it was only 2.5 mg/g for BSP.

The adsorption capacity of either BSP or BSA increased with the increasing pH values from 3 to 7 but slightly decreased further. This phenomenon can be attributed to the ionization of the adsorbent active sites as well as to the nature of the HA molecule. Indeed, hydrogen ions in weak acids typically enhance the adsorbent's positive charge, thereby increasing the adsorption of negatively charged HA molecules. Moreover, the conversion of HA from hydrophilic to hydrophobic together with the reduction of the ionic state facilitates the adsorption of this adsorbate in a weak acid solution. At low pH values, the concentration of H^+ ions is high, leading to flocculation of HA molecules thus lowering the adsorption capacity. When pH increases above 7, the electrostatic repulsion between the negative charge of the adsorbent surface and HA molecule increases, which in turn results in the decrease in the adsorption of HA molecules from solution to the solid phase, progressively (Liu et al. 2014). Similar investigations

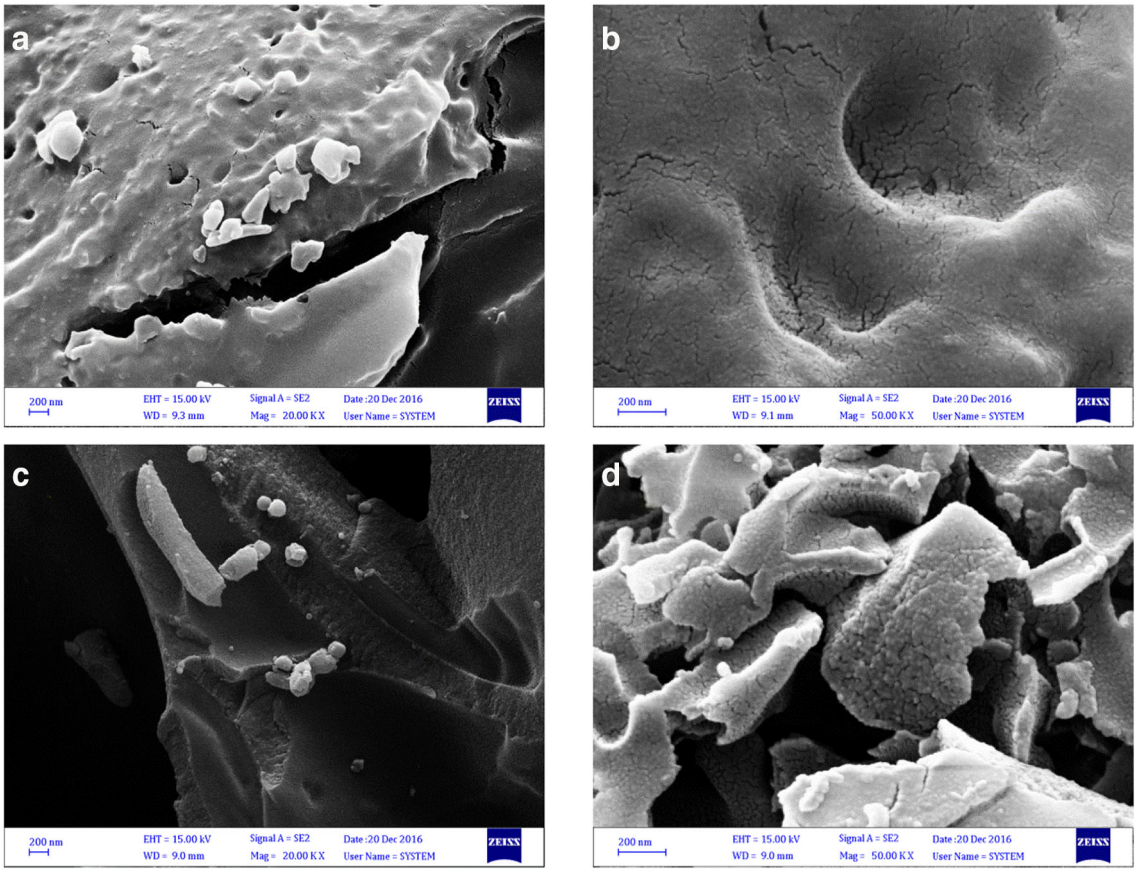

Fig. 2 SEM micrograph of adsorbents BSP before (**a**) and after (**b**) contacting with HA solution. Barberry Stem BSA before (**c**) and after (**d**) contacting with HA solution

have been reported during the removal of HA on other adsorbents like cross-linked chitosan (Ngah et al. 2008) and activated carbon (Chen et al. 2011).

Effect of reaction time at different HA concentrations

The analysis of the effect of reaction time in the test solutions was carried out at different initial HA concentration and the results obtained are plotted in Fig. 4. From the evolution curves, corresponding to the HA adsorption by BSP (Fig. 4a), one can state that the concentration of adsorbed HA molecule increases with prolonged time and subsequently reaches the equilibrium within 10 min. A further increase in the reaction time above 120 min had a low or insensible change in HA adsorption rate. However, the removal capacities under equilibrium condition increased from 2 to 15 mg/g with the further increase in HA concentration from 5 to 40 mg/L, because with increased HA concentration, the driving force for mass transfer also increases. The analysis also indicates that the adsorption of HA molecules, in the sizeable amount, was fast during the initial stage, due to the availability of a high number of uncovered reaction sites or groups on the outer surface of the adsorbent. These active sites provide a high probability for the HA molecules to sequester them. Subsequently, the required sites for the adsorption of HA are lacking, thus leading to the saturation condition. Indeed, the fast adsorption case at the beginning of the reaction time provides an advantageous property for the adsorbent to be an efficient material in the water and wastewater treatment applications (Li et al. 2017). Alternatively, the observation of fast adsorption of HA molecules onto BSP suggested that the adsorption of HA molecules in liquid–solid interfaces was mainly dominated by strong physical sorption. Likewise, the adsorption process of HA onto the barberry stem BSA occurs quickly and reached a plateau region within10 min of reaction time (see Fig. 4b). Additionally, the adsorption of HA by BSA significantly enhanced with the increase of the HA concentrations from 5 to 40 mg/L, and the ultimate uptake values were perceived, around 10 min of the experiment. The results also suggested that further increase in the reaction time above 10 min is not necessary to produce more adsorption yield; thus, in the subsequent experiments, this time was selected to ascertain the equilibrium of HA adsorption on both the adsorbents. Chang and Juang 2004 and Mohseni-Bandpi et al. 2016 reported similar results.

However, unusual phenomena were investigated in the adsorption uptake curves of HA onto BSA, in which, the adsorption rate was leveling off after 20 min of reaction time. But this

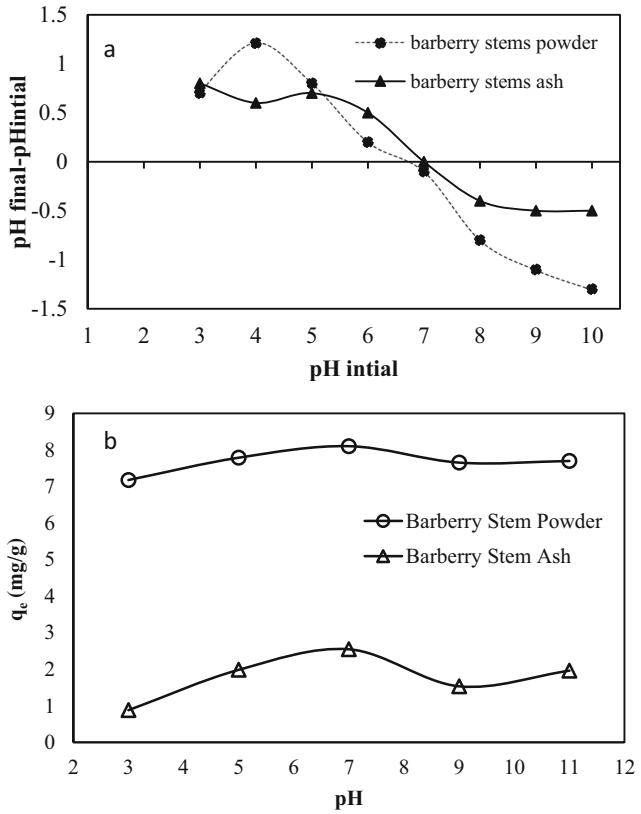

Fig. 3 Effect of pH on HA adsorption by BSP and BSA. **a** pHpzc of the biosorbents and **b** biosorption capacity and initial solution pH of HA (concentration of HA = 20 mg/L, reaction time = 60 min, dosage of adsorbent = 2 g/L)

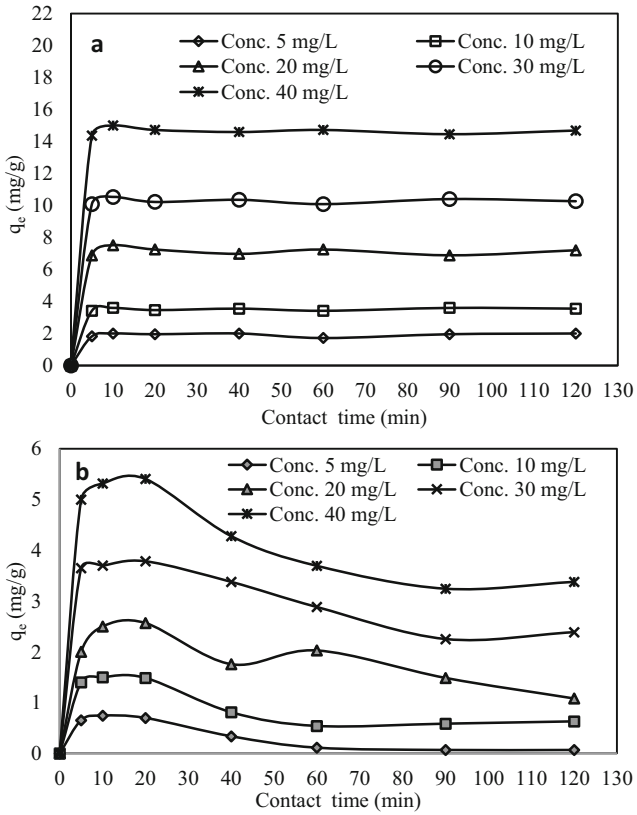

Fig. 4 Effect of concentration and reaction time on HA adsorption by BSP (**a**) and BSA (**b**) (pH = 7; dosage of adsorbent = 2 g/L; and HA concentrations of 5–40 mg/L).

phenomenon has not been addressed in the related studies, the reason being that the BSA material in itself produces turbid matters after a specific time of reaction. Therefore, the previously adsorbed HA molecules on the BSA may re-diffuse to the aqueous solution with the turbid matters leading to increase their concentration to a higher value than equilibrium level, thereby hindering the adsorption ability. Similar conclusions have been drawn by Malakootian and Kalankesh (2014) for HA adsorption onto silicon nanoparticles.

Effect of adsorbent dose

The HA adsorption uptake on BSP and BSA content was tested, as a function of these two adsorbents under constant conditions: initial HA concentration = 40 mg/L, pH = 7, and reaction time = 10 min. Figure 5, which depicts the result of this experiment, indicates that the increase in adsorbent content from 1 to 4 g/L reduced HA uptake abruptly from 24.1 to 5.7 mg/g and from 8 to 1.4 mg/g for BSP and BSA, respectively. Further, these results of decrease in the HA uptake values with the increase of BSP and BSA doses have been accredited to Eq. 1, which in turn elicits that an increase in the adsorbent dose in the aqueous solution reduces the amount of adsorbed pollutant per unit weight of dry solid. Physically, the aggregation of exchangeable binding sites of the used adsorbents for HA molecules can probably explain this observation (Samarghandi et al. 2015).

Effect of temperature

Several studies stated that temperature is also a crucial factor that might affect the adsorption process (Sulaymon et al.

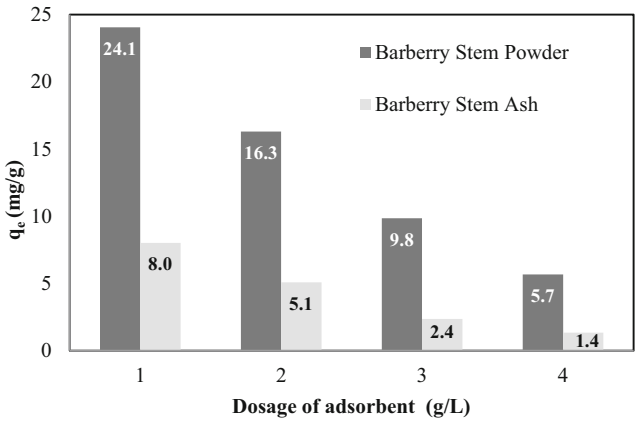

Fig. 5 Effect of BSP and BSA content on the HA uptake (initial HA concentration = 40 mg/L, pH = 7, and reaction time = 10 min)

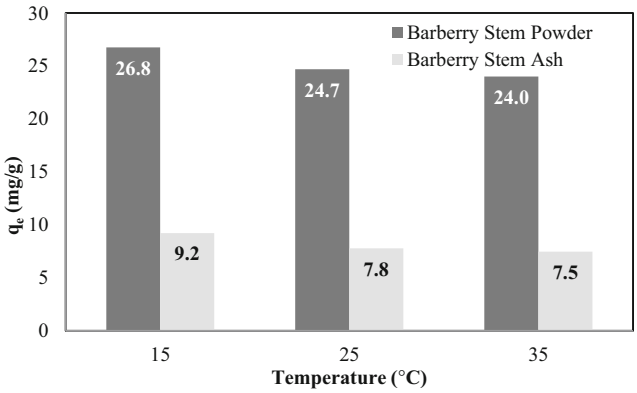

Fig. 6 Effect of temperature on removal of HA on BSP and BSA (pH = 7, concentration of HA = 40 mg/L, dosage of adsorbent = 1 g/L, and reaction time = 10 min)

2014). Further, to study the effect of temperature on HA adsorption, experiments were carried out at different solution temperatures such as 15, 25, and 35 °C, while fixing the other parameter at the optimized values given from previous experiments (see Fig. 6). Thus, with an increase in temperature, no significant change of HA removal was observed. Indeed, the HA uptake on two studied adsorbents was decreased slightly, by less than 3%, while at a temperature of 15 °C, the maximum HA uptake was established. Therefore, one can deduce that the variation of solution temperature had minimal effect on the HA adsorption. Alternatively, the reason for the reduction in the HA adsorption yield at high temperature may be the destruction of the adsorbent active sites (Sulaymon et al. 2014; Saleem et al. 2007). Additionally, when the temperature increased, the thickness of the boundary layer of the adsorbent might be reduced as a result of reduced viscosity of the solution (Bulut et al. 2012). Such reduction in the boundary layer permits the adsorbed molecules to undergo desorption into the solution (Priya and Radha 2015).

The results of the thermodynamic investigation of the adsorption process and its related parameters are reported in Table 1. The values of $\Delta G°$ for adsorption of HA onto BSP at different temperatures were negative demonstrating a spontaneous adsorption reaction, while the adsorption nature of HA onto BSA was non-spontaneous as positive values of ΔG° were determined. However, the negative numbers of both $\Delta H°$ and $\Delta S°$ demonstrated the exothermic nature of HA adsorption onto BSP and BSA and a decrease in randomness during the interaction at the liquid–solid phase (Kamranifar and Naghizadeh 2017).

Adsorption isotherms

The term isotherm is used to estimate the interaction in a liquid–solid medium between the amounts of retained and non-retained adsorbate on an adsorbent, upon reaching equilibrium state at constant temperature (Brouers and Al-Musawi 2015). Therefore, the analysis and simulation of the experimental isothermal data with the mathematical models is considered as an essential approach in an engineered treatment system to determine the adsorption capacity of an adsorbent for a specific pollutant from aqueous solutions. In this study, the well-defined mathematical models of Langmuir, Freundlich, BET, Temkin, and Dubinin-Radushkevich have been applied to model the isothermal data of HA adsorption. The models' parameters listed in Table 2 were determined using nonlinear modeling algorithms built in the STATISTICA program.

The results of the correlation coefficient (R^2) given in Table 2 indicate that both Langmuir and Freundlich models are adapted satisfactorily, for the fitting of HA adsorption isotherms on the BSP. Additionally, the maximum HA adsorption capacity, according to the Langmuir model, was in the order of BSP > BSA. These results suggest that converting BSP to BSA form did not improve the HA adsorption yield, which can be reasoned by pointing out that during the process of BSA preparation from virgin BSP, some of the active groups responsible for the adsorption of HA molecules were deactivated. Moreover, from the values of K_f Freundlich constant, it can be concluded that BSP has a higher affinity toward HA molecules than BSA. The values of n were > 1 for both adsorbents, suggesting that the amount of adsorption will approach a limit for HA (Zhang and Bai 2003). Further, the isotherm study enlightens that the Freundlich and Langmuir isotherms were the best fit for the isothermal data of HA adsorption onto BSP and BSA, respectively. As a result, the

Table 1 Thermodynamic analysis for the HA adsorption onto BSP and BSA

Adsorbent	T (°C)	q_e (mg/g)	Thermodynamic parameters		
			$\Delta G°$ (kJ/mol)	$\Delta H°$ (kJ/mol)	$\Delta S°$ (J/mol K)
BSP	15	26.8	− 1.68	− 11.01	− 32.57
	25	24.7	− 1.18		
	35	24.0	− 1.04		
BSA	15	9.2	2.88	− 9.89	− 44.56
	25	7.8	3.52		
	35	7.5	3.76		

Table 2 Parameters of adsorption isotherm for the HA adsorption onto BSP and BSA

Model	Constants	BSP	BSA
Langmuir	q_{max} (mg/g)	20.220	16.950
	K_L (L/mg)	0.106	0.012
	R_L	0.190	0.670
	R^2	0.963	0.988
Freundlich	K_f (mg/g)	1.821	0.220
	$1/n$	0.850	0.910
	n	1.180	1.100
	R^2	0.979	0.961
BET	1/A.Xm	0.200	5.470
	$(A-1)/(A.Xm)$	0.530	5.170
	A	1.110	29.300
	Xm	2.100	5.670
	R^2	0.350	0.028
Temkin	A_T, L/mg	1.090	0.320
	b_T	486.350	1241.71
	B	5.091	2.000
	R^2	0.841	0.833
Dubinin–Radushkevich	β, mole^2/kJ^2	6E−07	5E−06
	E, kJ/mole	0.910	0.320
	q_m, mg/g	9.450	3.470
	R^2	0.747	0.801

multilayer adsorption was demonstrated for HA molecules adsorption onto surfaces of BSP, thereby indicating that the HA molecules can bind to more than one surface, while a monolayer adsorption process probably dominated for HA adsorption onto the BSA surface. Based on the results of Dubinin–Radushkevich model analysis (Table 2), it can be concluded that the adsorption process of HA onto the two adsorbents is probably physical in nature, where all the determined E values were less than 8 kJ/mol (Regassa et al. 2016).

Kinetic study

In the present investigation, the applicability of pseudo-first-order and pseudo-second-order kinetic models for the analysis of HA adsorption kinetics was tested and validated. As mentioned earlier, the data obtained from the study of the effect of reaction time experiments were employed, for the kinetic study. Further, the nonlinear analysis results of these models with the experimental data are reported in Table 3, which showed a good agreement between the experimental data and the pseudo-second-order model as indicated by the satisfactory R^2 values (close to 1). Thus, this kinetic model is consistent with the trend of adsorption rate at different concentrations of HA in the entire range studied. Moreover, the calculated uptake values from the pseudo-second-order kinetic model were more consistent with the experimental kinetic values than those calculated from the pseudo-first-order kinetic model. Such trends suggested the occurrence of chemosorption process between HA molecules and adsorbents sites. This finding is not consistent with the obtained results from the isotherm study. Additionally, it was also observed in Table 3 that the uptake values at all HA concentrations (considered for the study), were higher in the case of BSP than in the BSA material which implies that HA molecules have more affinity for the surface sites of BSP than the BSA reactive groups.

Conclusion

In this study, the investigated of the adsorption capacity of barberry stem powder (labeled as BSP) and barberry stem ash (labeled as BSA) towards humic acid (HA) was conducted in a batch mode. Further, to optimize the HA adsorption process, the effects of different experimental conditions in term of pH, reaction time, initial HA concentration, adsorbent content,

Table 3 Parameters of adsorption kinetics for the HA adsorption on BSP and BSA with different HA concentration

			Pseudo-first order			Pseudo-second order		
Adsorbent	C_0 (mg/L)	q_e, exp (mg/g)	K_1 (min^{-1})	q_e, cal (mg/g)	R^2	K_2 (g/mg min)	q_e, cal (mg/g)	R^2
BSP	5	3.10	0.001	1.141	0.018	0.103	2.00	0.990
	10	4.61	0.001	1.110	0.029	0.386	3.60	0.999
	20	8.50	0.002	1.311	0.140	2.788	7.11	0.999
	30	11.51	0.001	1.253	0.051	1.429	10.30	0.999
	40	16.00	0.001	1.291	0.131	0.973	14.61	0.999
BSA	5	1.72	0.005	1.035	0.833	0.001	0.12	0.936
	10	2.51	0.004	1.454	0.325	0.020	0.60	0.981
	20	3.60	0.004	1.684	0.185	0.010	1.24	0.931
	30	4.81	0.007	1.232	0.638	0.016	2.33	0.983
	40	6.40	0.010	1.161	0.801	0.014	3.24	0.998

and temperature were thoroughly examined. Results demonstrated that HA was substantially removed, at conditions of pH near neutral, reaction time = 10 min, temperature = 15 °C, initial HA concentration = 40 mg/L, and adsorbent amount = 1.0 g/L. The adsorption efficiency of HA onto BSP and BSA were not affected greatly by the varying pH values from 3 to 11 and temperature from 15 to 35 °C. However, the results indicated that the adsorption process of HA molecules extremely depends on the initial concentration of HA and adsorbent dose. The experiment of the effects of reaction time reported fast HA kinetic profile at the beginning of the reaction time followed by the attainment of adsorption equilibrium within the first 10 min. Moreover, in the case of the BSA material, the unusual trend of decrease in the adsorption rate was highlighted for HA adsorption, after 20 min of the reaction time. Additionally, the kinetic study highlighted that the pseudo-second-order model fits better with the experimental data of HA kinetics than the pseudo-first-order model. In addition, the analysis of the isotherm indicated that the HA adsorption process is in agreement with both Langmuir and Freundlich isotherms. The maximum adsorption Langmuir uptakes of BSP and BSA were found to be 20.220 and 16.950 mg/g, respectively. The analysis of the Dubinin–Radushkevich isotherm model demonstrated that adsorption of HA molecules on the surface sites of BSP and BSA follows the physical sorption process. Moreover, the results indicated that the adsorption nature of HA molecules was exothermic, as indicated by the thermodynamic study. Generally, BSP exhibited adsorptive performance better than the BSA for the adsorption of HA from the aqueous solution. In future studies, the FTIR and XRD analysis should also be examined.

Acknowledgments The authors express their gratitude to colleagues at the research laboratory/Faculty of Health/Birjand University of Medical Sciences (Iran) for their spiritual support at various stages of this study.

References

Anirudhan TS, Ramachandran M (2007) Surfactant-modified bentonite as adsorbent for the removal of humic acid from wastewaters. Appl Clay Sci 35(3–4):276–281

Babi K, Koumenides K, Nikolaou A, Makri C, Tzoumerkas F, Lekkas T (2007) Pilot study of the removal of THMs, HAAs and DOC from drinking water by GAC adsorption. Desalination. 210(1-3):215–224

Balsamo M, Montagnaro F (2015) Fractal-like Vermeulen kinetic equation for the description of diffusion-controlled adsorption dynamics. J Phys Chem C 119:8781–8785

Bazrafshan E, Biglari H, Mahvi AH (2012) Humic acid removal from aqueous environments by electrocoagulation process using iron electrodes. J Chem 9(4):2453–2461

Brouers F, Al-Musawi TJ (2015) On the optimum use of isotherm model for the characterization of biosorption of lead onto algae. J Mol Liq 212:46–51

Brouers F, Al-Musawi TJ (2018) Brouers-Sotolongo fractal kinetics versus fractional derivative kinetics: a new strategy to analyze the pollutants sorption kinetics in porous materials. Hazard Mater 350: 162–168

Bulut Y, Gul A, Baysal Z, Alkan H (2012) Absorption of ni(II) from aqueous solution by Bacillus subtilis. Desalin Water Treat 49:74–80

Chang M-Y, Juang R-S (2004) Adsorption of tannic acid, humic acid, and dyes from water using the composite of chitosan and activated clay. J Colloid Interface Sci 278(1):18–25

Chen H, Zhao J, Wu J, Dai G (2011) Isotherm, thermodynamic, kinetics and adsorption mechanism studies of methyl orange by surfactant modified silkworm exuviae. J Hazard Mater 192(1):246–254

Dehghani MH, Nazmara S, Zahedi A, Rezanasab M, Nikfar E, Oskoei V (2015) Efficiency rate of photocatalytic UV/ZnO in removing humic acid from aqueous solution. Journal of Mazandaran University of Medical Sciences (JMUMS) 24(120):264–277

Dong C, Chen W, Liu C (2014) Preparation of novel magnetic chitosan nanoparticle and its application for removal of humic acid from aqueous solution. Appl Surf Sci 292:1067–1076

Doulia D, Leodopoulos C, Gimouhopoulos K, Rigas F (2009) Adsorption of humic acid on acid-activated Greek bentonite. J Colloid Interface Sci 340(2):131–141

Freundlich HMF (1906) Over the adsorption in solution. J Phys Chem 57: 385–407

Gasser MS, Mohsen HT, Aly HF (2008) Humic acid adsorption onto Mg/Fe layered double hydroxide. Colloids Surf A Physicochem Eng Asp 331:195–201

Hassani A, Kiransan M, Soltani RDC, Khataee A, Karaca S (2015) Optimization of the adsorption of a textile dye onto nanoclay using a central composite design. Turk J Chem 39:734–749

Ho YS, Mckay G (2000) The kinetics of sorption of divalent metal ions onto sphagnum moss peat. Water Res 34(3):735–742

Kamranifar M, Naghizadeh A (2017) Montmorillonite nanoparticles in removal of textile dyes from aqueous solutions: study of kinetics and thermodynamics. Iran J Chem Chem Eng 36:127–137

Lagergren S (1898) About the theory of so-called adsorption of soluble substances. Kungliga Svenska Vetenskapsakademiens Handlingar (in Swedish) 24:1–39

Langmuir I (1918) The adsorption of gases on plane surfaces of glass, mica and platinum. J Am Chem Soc 40:1361–1403

Li S, He M, Li Z, Li D, Pan Z (2017) Removal of humic acid from aqueous solution by magnetic multi-walled carbon nanotubes decorated with calcium. J Mol Liq 230:520–528

Liu S, Lim M, Fabris R, Chow C, Chiang K, Drikas M, Amal R (2008) Removal of humic acid using TiO 2 photocatalytic process–fractionation and molecular weight characterisation studies. Chemosphere. 72(2):263–271

Liu S, Lim M, Amal R (2014) TiO_2-coated natural zeolite: rapid humic acid adsorption and effective photocatalytic regeneration. Chem Eng Sci 105:46–52

Low SC, Liping C, Hee LS (2008) Water softening using a generic low cost nano-filtration membrane. Desalination. 221(1):168–173

Malakootian M, Kalankesh RL (2014) Assessing the performance of silicon nanoparticles in adsorption of Humic acid in water. Iranian Journal of Health and Environment. 6(4):535–544

Mansoury M, Godini H, Shams Khorramabadi G (2015) Photocatalytic removal of natural organic matter from aqueous solutions using zinc oxide nanoparticles immobilized on glass. Iran J Health Environ 8(2):181–190

Milonjic SK (2007) A consideration of the correct calculation of thermodynamic parameters of adsorption. J Serb Chem Soc 72(12):1363–1367

Mohammed AA, Brouers F, Samaka IS, Al-Musawi TJ (2018) Role of Fe3O4 magnetite nanoparticles used to coat bentonite in zinc(II) ions sequestration. Environ Nanotechnol Monit Manag 10:17–27

Mohammed AA, Najim AA, Al-Musawi TJ, Alwared AI (2019) Adsorptive performance of a mixture of three nonliving algae

classes for nickel remediation in synthesized wastewater. J Environ Health Sci Eng. https://doi.org/10.1007/s40201-019-00367-w

Mohseni-Bandpi A, Al-Musawi TJ, Ghahramani E, Zarrabi M, Mohebi S, Vahed SA (2016) Improvement of zeolite adsorption capacity for cephalexin by coating with magnetic Fe3O4 nanoparticles. J Mol Liq 218:615–624

Naghizadeh A, Nasseri S, Rashidi A, Kalantary RR, Nabizadeh R, Mahvi A (2013) Adsorption kinetics and thermodynamics of hydrophobic natural organic matter (NOM) removal from aqueous solution by multi-wall carbon nanotubes. Water Sci Technol Water Supply 13(2):273–285

Naghizadeh A, Shahabi H, Ghasemi F, Zarei A (2016) Synthesis of walnut shell modified with titanium dioxide and zinc oxide nanoparticles for efficient removal of humic acid from aqueous solutions. J Water Health 14(6):989–997

Ngah WW, Hanafiah M, Yong S (2008) Adsorption of humic acid from aqueous solutions on crosslinked chitosan–epichlorohydrin beads: kinetics and isotherm studies. Colloids Surf B: Biointerfaces 65(1): 18–24

Ngah WW, Fatinathan S, Yosop N (2011) Isotherm and kinetic studies on the adsorption of humic acid onto chitosan-H2SO4 beads. Desalination. 272(1):293–300

Noroozi R, Al-Musawi TJ, Kazemian H, Kalhori EM, Zarrabi M (2018) Removal of cyanide using surface-modified Linde Type-A zeolite nanoparticles as an efficient and eco-friendly material. Water Process Eng 21:44–51

Priya SS, Radha K (2015) Equilibrium, isotherm, kinetic and thermodynamic adsorption studies of tetracycline hydrochloride onto commercial grade granular activated carbon. Int J Pharm Pharm Sci 7(1):42–51

Regassa M, Melak F, Birke W, Alemayehu E (2016) Defluoridation of water using natural and activated coal. IARJSET. 3(1):1–7

Rodrigues DAS, Moura JM, Dotto GL, Jr TRS, Pinto LAA (2018) Preparation, characterization and dye adsorption/reuse of chitosanvanadate films. J Polym Environ 26(7):2917–2924

Saleem M, Pirzada T, Qadeer R (2007) Sorption of acid violet 17 and direct red 80 dyes on cotton fiber from aqueous solutions. J Colloids Surf A Physicochem Eng Asp 292:246–250

Samarghandi M, Al-Musawi T, Mohseni-Bandpi A, Zarrabi M (2015) Adsorption of cephalexin from aqueous solution using natural zeolite and zeolite coated with manganese oxide nanoparticles. J Mol Liq 211:431–441

Şeker A, Shahwan A, Eroğlu AE, Yılmaz S, Demirel Z, Dalay MC (2008) Equilibrium, thermodynamic and kinetic studies for the biosorption of aqueous lead (II), cadmium (II) and nickel (II) ions on Spirulina platensis. J Hazard Mater 154:973–980

Selcuk H, Bekbolet M (2008) Photocatalytic and photoelectrocatalytic humic acid removal and selectivity of TiO_2 coated photoanode. Chemosphere. 73(5):854–868

Sulaymon A, Mohammed A, Al-Musawi TJ (2014) Comparative study of removal of cadmium (II) and chromium (III) ions from aqueous solution using low-cost biosorbent. Int J Chem React Eng 12(1):1–10

Uyak V, Ozdemir K, Toroz I (2008) Seasonal variations of disinfection by-product precursors profile and their removal through surface water treatment plants. Sci Total Environ 390(2):417–424

Wang XS, Zhou Y, Jiang Y, Sun C (2008) The removal of basic dyes from aqueous solutions using agricultural by-products. J Hazard Mater 157(2):374–385

Wang J, Bi L, Ji Y, Ma H, Yin X (2014) Removal of humic acid from aqueous solution by magnetically separable polyaniline: adsorption behavior and mechanism. J Colloid Interface Sci 430:140–146

Zhang Z, Bai R (2003) Mechanisms and kinetics of humic acid adsorption onto chitosan-coated granules. J Colloid Interface Sci 264:30–38

Zhang X, Minear RA (2006) Formation, adsorption and separation of high molecular weight disinfection byproducts resulting from chlorination of aquatic humic substances. Water Res 40(2):221–230

Zhang J, Gong J-L, Zenga G-M, Ou X-M, Jiang Y, Chang Y-N, Guo M, Zhang C, Liu HY (2016) Simultaneous removal of humic acid/fulvic acid and lead from landfill leachate using magnetic graphene oxide. Appl Surf Sci 370:335–350

Zulfikar M, Novita E, Hertadi R, Djajanti S (2013) Removal of humic acid from peat water using untreated powdered eggshell as a low cost adsorbent. Int J Environ Sci Technol 10(6):1357–1366